Additive Manufacturing 36 (2020) 101409

Contents lists available at ScienceDirect

Additive Manufacturing

journal homepage: www.elsevier.com/locate/addma

Research Paper

Flash ablation metallization of conductive thermoplastics

Jorge A. Cardenas[a,b], Harvey Tsang[c], Huayu Tong[d], Hattan Abuzaid[b], Katherine Price[c], Mutya A. Cruz[d], Benjamin J. Wiley[d], Aaron D. Franklin[a,d], Nathan Lazarus[c,*]

[a] ORAU Fellowship Program at Army Research Lab, Adelphi, MD, 20783, USA
[b] Department of Electrical and Computer Engineering, Duke University, Durham, NC, 27708, USA
[c] Army Research Lab, Adelphi, MD, 20783, USA
[d] Department of Chemistry, Duke University, Durham, NC, 27708, USA

ARTICLE INFO

Keywords:
Conductive thermoplastic
3D printing
Printed electronics
Fused filament fabrication
Photonic annealing

ABSTRACT

Fused filament fabrication (FFF) is the most widely available 3D printing technology. Recently, a variety of conductive thermoplastic filaments have become commercially available, allowing printing of electronic structures using the technology. However, the contact interface and conductivity of these filaments after printing remains relatively poor, the latter of which is typically at least four orders of magnitude lower than bulk metal conductors. While several post-processing approaches exist to enhance conductivity, they are either user-intensive, time consuming, or cannot easily be integrated in-line with the rest of the printing process. In this work, we demonstrate that exposing conductive composite thermoplastic films (3D printed or solution-cast) to high-intensity pulsed light increases their conductance by up to two orders of magnitude in a manner that is fast, non-contact, and potentially in-line. This process, referred to as flash ablation metallization (FAM), is found to vaporize the thermoplastic matrix on the top surface of a composite film, leaving behind a metal-dense surface layer. The technique was found to be effective for a variety of commercial and custom-made conductive thermoplastic composites, with the largest response found in Electrifi, a commercial filament consisting of copper particle loading in a biodegradable polyester. 3D-printed circuit boards were constructed with and without FAM exposure, with exposed circuits exhibiting reduced operating voltages as well as improvements in reliability.

1. Introduction

Multi-material additive manufacturing (AM) is a maturing field of production that allows for the creation of highly customized parts and systems in a low-cost and rapid manner [1]. Over the past 20 years, significant time and research has been invested into the development of materials possessing electronic functionality that are compatible with AM processes [2–5]. These new materials have resulted in the development of printed electronics that have found applications in passive components, low-cost RFID tags, antenna, sensors, printed circuit boards (PCBs) and packaging [6–9]. Despite the ongoing growth of printed electronics and functional inks, these advances have largely excluded the most widely available of AM methods: fused filament fabrication (FFF), which has the potential to enable the widespread use of 3D-printed electronics. Whereas methods such as inkjet [10], screen [11], and direct-write printing [12] have long been capable of printing high-quality conductive, dielectric, and even semiconducting inks and pastes [13–15], printing electronically functional filaments has been limited for FFF due to restrictions in compatible thermoplastic and composite materials [16]. Only recently have conductive composite thermoplastic filaments become commercially available [17,18], which have resulted in demonstrations of 3D FFF printed components [19], antennas [20], printed circuit boards, and metamaterials [22].

Outside of AM, conductive thermoplastic and polymer composites have long been used in electromagnetic interference (EMI) shielding [23] and thermal dissipation [24] applications. In a similar manner to previous work on composites, relatively high conductivity has been imbued in FFF-compatible thermoplastics by loading them with a suspension of conductive particulates to create an extrudable filament [25,26]. Conductive carbon particulates, either in the form of carbon black or graphene, are commonly used in commercial conductive filaments, however, these filaments exhibit poor conductivity, with resistivity values ranging from 0.21–120 Ω cm [18,26,27]. In contrast, filaments loaded with metallic particles, including Electrifi, a commercially available copper flake-based filament, or similar silver-coated copper nanowire-based filaments, have exhibited resistivities as low as 0.002 Ω cm and are the most conductive filaments reported to date [19,26]. However, these conductive filaments rely on long percolation

* Corresponding author.
E-mail address: nathan.lazarus2.civ@mail.mil (N. Lazarus).

https://doi.org/10.1016/j.addma.2020.101409
Received 3 March 2020; Received in revised form 15 June 2020; Accepted 19 June 2020
Available online 24 June 2020
2214-8604/ Published by Elsevier B.V.

paths through a metallic particle network that is embedded in a highly resistive thermoplastic at a relatively low volume fraction, resulting in composite filaments that are still 10^3 times more resistive than bulk metals and at least 10^2 times more resistive than most commercial conductive inks or pastes. [28,29]

In addition to these shortcomings in conductivity, conductive filaments also possess a number of other non-ideal thermal and electrical characteristics that further obstruct their widespread use. One such shortcoming is poor electrical contact, which is primarily exhibited by the metallic particle composite thermoplastics due to the metallic particles being imbedded within the thermoplastic rather than at the surface [17,26]. Thermally, the conductivity is also quite sensitive to, and significantly degrades at, higher temperatures [19,26,30]. This can result in printed film conductivities that are an order of magnitude lower than initial filament conductivities once the filament has been extruded from an FFF nozzle. Additionally, this same thermal behavior also prevents these 3D printed filaments from being thermally cured post-process, which is the most common post-process method for improving printed inks or pastes. Commonly used post-process methods that have been shown to improve the conductivity of FFF-printed filaments are electro- and electroless plating [20,31,32]. Although these methods can deposit a layer of highly conductive bulk metal onto a printed filament, it is a highly user intensive post-process method that requires external handling away from the printer, is time consuming (takes several hours), and involves submerging the part in electrolytic solution. A much more ideal post-process method for enhancing conductivity of a thermoplastic filament, such as a photonic process, would be rapid, non-contact, and take place in-line with the rest of the printing process in an autonomous manner.

In this work, we demonstrate that exposing conductive composite thermoplastic films, both 3D printed and solution-cast, to high-intensity pulsed light increases their conductance by up to two orders of magnitude. A Novacentrix Pulseforge® 1200, a tool which has typically been used to photonically anneal liquid inks and pastes, [33–35] is used for the first time to expose conductive composite thermoplastic to high-intensity pulses of white light emitted from a flash lamp. This process, referred to as flash ablation metallization (FAM), is found to quickly vaporize the topmost layer of thermoplastic, leaving behind a metallized surface layer, without significantly raising the film's internal temperature, such that the negative effects of thermal sintering are not reproduced. High-intensity pulsed light is generally found to enhance a variety of conductive composite thermoplastics, both commercially available and custom-made. Primary focus in this work is given to Electrifi (Multi3D LLC) since it is the most conductive filament available on the commercial market in addition to showing the greatest improvement in conductance in response to high intensity light exposure. Surface and cross-sectional scanning electron microscopy (SEM) images of Electrifi, as well as optical images, were used to characterize its changes in morphology and particle distribution throughout 3D printed films, and 4-point probe resistance measurements were used to characterize films before and after various exposure conditions. Additionally, x-ray photoelectron spectroscopy (XPS) and energy dispersive x-ray spectroscopy (EDS) were used to determine changes in surface composition. To demonstrate the immediate potential for pulsed-light to be used in functional 3D-printed electronic applications, 3D-printed circuit boards were constructed on acrylonitrile butadiene styrene (ABS) substrates with and without light exposure, with the exposed samples exhibiting significant improvements in circuit functionality and reliability. The FAM technique demonstrated here opens up the possibility for significant advancements to be made in FFF-printed electronics as well as applications outside of additive manufacturing involving conductive thermoplastic composites, such as EMI shielding and thermal dissipation.

2. Results and discussion

Unless otherwise noted, the samples produced in this work were printed from a commercially available dual extrusion FFF 3D printer (Makerbot Replicator 2X), which operates by extruding melted thermoplastic through a finely tipped nozzle to build parts in three dimensions in a layer-by-layer manner. One nozzle on the FFF printer was used to print non-conducting substrate material (green or yellow ABS), while the other nozzle printed conductive composite filament. Although Electrifi was the most heavily used conductive filament throughout this work, a number of other conductive thermoplastic composites were also studied, including custom-made thermoplastics, which will be outlined further below.

Prior to assessing the effects of pulsed-light exposure on 3D printed parts, 0.2 mm thick 4-point probe test structures were printed from Electrifi onto polyimide at room temperature, which exhibited sheet resistances as low as 4 Ω/sq prior to exposure, corresponding to resistivities as low as 0.08 Ω cm. However, the average sheet resistance of 0.3 mm thick as-printed Electrifi was approximately 20 Ω/sq when printed on ABS. Thickness of test specimens were chosen on each substrate to be as thin as possible while being thick enough to be reliably continuous from print to print. Unless otherwise specified, all test specimens printed on ABS were 0.3 mm thick. It should be noted that the resistivity of the as-printed Electrifi samples prepared in this work are considerably higher than the 0.006 Ω cm metric that is reported by Multi3d LLC due to the thermal energy absorbed by the filament from the extrusion process, the surrounding ABS substrate, and the heated build plate, which is consistent with the results reported in Multi3d's supplementary product literature [17].

After test coupons (consisting of three adjacent 4-point Kelvin probe structures on ABS) were printed, they were manually moved from the 3D printer to a Novacentrix PulseForge® 1200 for photonic processing. A schematic diagram of the PulseForge® lamp and sample setup is illustrated in Fig. 1A, highlighting the general exposure process, which lasted only a matter of milliseconds. PulseForge® tools consist of a xenon flash lamp that emits white light generated from an arc plasma within the lamp [36]. Prior to exposure, the energy released from the flash lamp is stored in a capacitor bank, which a user can arbitrarily vary by charging the capacitor bank to voltage values within the limits of the tool (in the case of the Pulseforge® 1200, the limits are 200 V–450 V). The Pulseforge® is then able to release this stored energy through the flash lamp using one or multiple pulses of light at a user-defined pulse width. Calculated power density profiles that are emitted from the flash lamp are plotted in Fig. 1B as a function of time, which shows that increasing the bank voltage corresponds to a larger power density profile. These profiles are modelled by the Pulseforge software itself, while lamp current, photodiodes, and a bolometer are used to calibrate the tool and confirm its calculated power profiles. Elevated surface temperatures that result from these increasing power density profiles are conceptually plotted in Fig. 1C in a qualitative manner (with no y-axis data included), showing that increasing surface temperatures result from increasing power density profiles. These curves were generated by simulating ABS being exposed to pulses with power density profiles seen in Fig. 1B. The simulation software used was SimPulse®, a one-dimensional heat transfer simulation software provided by the Pulseforge manufacturer, Novacentrix. It should be noted that this simulation does not take thermoplastic ablation into account in its assumptions [37].

Immediately after exposure, small but distinct visual changes are evident on the surface of the conductive thermoplastics, including a shift from a lustrous surface texture to a rough, more diffuse texture. Fig. 1D shows an optical image of exposed and unexposed traces of Electrifi printed onto ABS, where a slight color shift to a more copper-like bronze finish can be seen after exposure, in addition to surface roughening. At the microscale, surface roughness is heightened as a result of greater density of metal particles. However, at the millimeter-

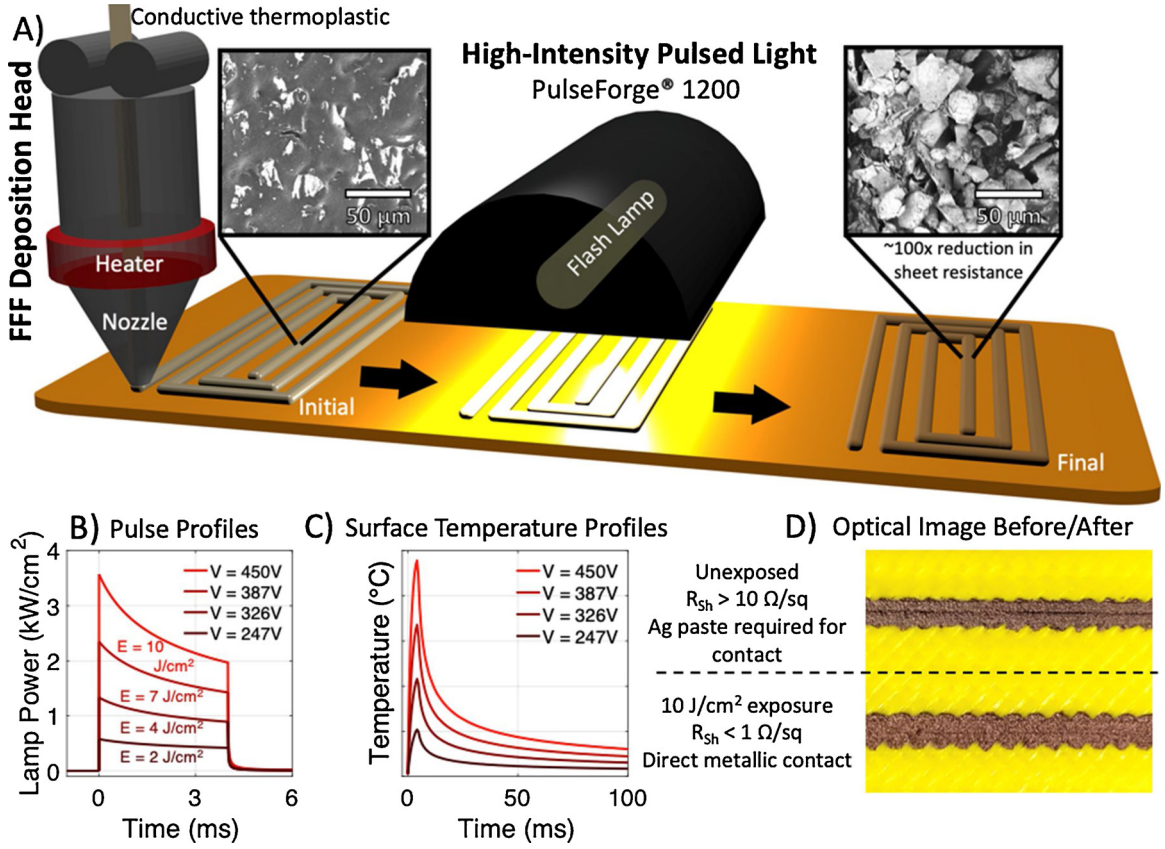

Fig. 1. Schematic diagram of the FFF printing and pulsed-light exposure process. A) Illustration of the FFF printing and pulsed light exposure process with filament surface morphology highlighted before and after exposure. B) Calculated power profiles emitted from the flash lamp at various capacitor bank voltages. C) Qualitative plot of simulated surface temperature values on ABS during and after exposure. D) Optical comparison of as-printed versus exposed filament.

scale, hatches on the printed FFF surface become slightly smoother as the heat from the flash momentarily melts and reforms the top layer. SEM images were used to assess the changes in surface morphology of Electrifi, which can be seen in the insets of Fig. 1A as well as Fig. 2A-C, where it was found that exposed samples had a much more copper-dense surface. In the case of unexposed samples (see Fig. 2A), much of the surface consisted of thermoplastic, with only small areas of copper protruding out of the plastic, which explains Electrifi's poor ability to be directly probed through mechanical contact with another conductor, and leads to the need for silver paste to be added in the contact areas for interfacing [17]. In contrast, after exposure, the filament can be directly probed with another conductor with stable electrical contact.

To assess the cross-section of printed lines, test coupons were cast in a solid epoxy, then sanded and polished down to produce smooth cross-sections to be imaged with an optical microscope. These images can be seen in Fig. 2G-I. Fig. 2G depicts the case of unexposed thermoplastic, showing a smooth thermoplastic surface with little to no copper-flakes protruding out of the surface, consistent with the previously mentioned SEM images. In contrast, Fig. 2I depicts the case of exposed filament, which exhibits significant restructuring of the copper flakes at the surface, with many of the flakes protruding upwards, out of the thermoplastic. However, there was no significant restructuring of the flakes within the bulk of the thermoplastic, suggesting that the effects of pulsed-light exposure only penetrates $10-50$ µm beneath the surface.

Mass measurements were carried out using a microgram scale, where it was found that the composite filament's mass significantly decreased after each pulse. 2.25 cm^2 of ABS and Electrifi were printed onto glass slides, as depicted in Supplementary Fig. 1A, and their mass was measured before and after 5 high-intensity exposures. It was found that Electrifi's mass reduced by an average of 440 ± 10 µg/cm^2 after each exposure, indicating that the topmost layer of thermoplastic is being ablated away. Meanwhile, the mass of ABS remained relatively constant after each exposure, indicating that little to no ABS is being ablated, likely because ABS is a higher temperature thermoplastic compared to the biodegradable polyester that Electrifi consists of. Furthermore, it can be seen in the side-view SEM images shown in Figs. 2D-F that some copper particulates have been ejected from the conductive filament onto the surrounding ABS as a result of exposure, whereas as-printed and thermally cured samples show no such effects. It was also found that the flakes that remained on the exposed films were loosely held together and could be stripped off using tape, which resulted in a 50 % increase in resistance after each tape test. The flakes are, however, held sufficiently in place that elastomer encapsulation to maintain the higher conductivity is possible, and a number of encapsulation methods were successfully tested. Sealing the test coupons in an electronic packaging silicone (as depicted in Supplementary Figure S2A) overnight at room temperature successfully protected the exposed films without increasing their sheet resistance. As an alternative protection method, additional layers of ABS could be printed over the exposed Electrifi (as depicted in Supplementary Figure S2B), though the resulting films were slightly more resistive due to the thermal energy imparted on them by the ABS nozzle.

To better understand the mechanism resulting in conductivity increase instead of reduction, as in the case of thermal treatment, thermally treated samples were also prepared. Electrifi samples were printed and thermally cured for 30 min at 180 °C. The resulting samples exhibited ~10^6 Ω/sq sheet resistance values, in comparison to the 20 Ω/sq values for as-printed samples and 0.3 Ω/sq for photonically treated samples. Despite the significant increase in resistance of the thermally cured samples, more of the copper revealed itself at the surface of the composite, as seen in the SEM image of Fig. 2B. However, the cross-sectional optical images shown in Fig. 2H depict much larger

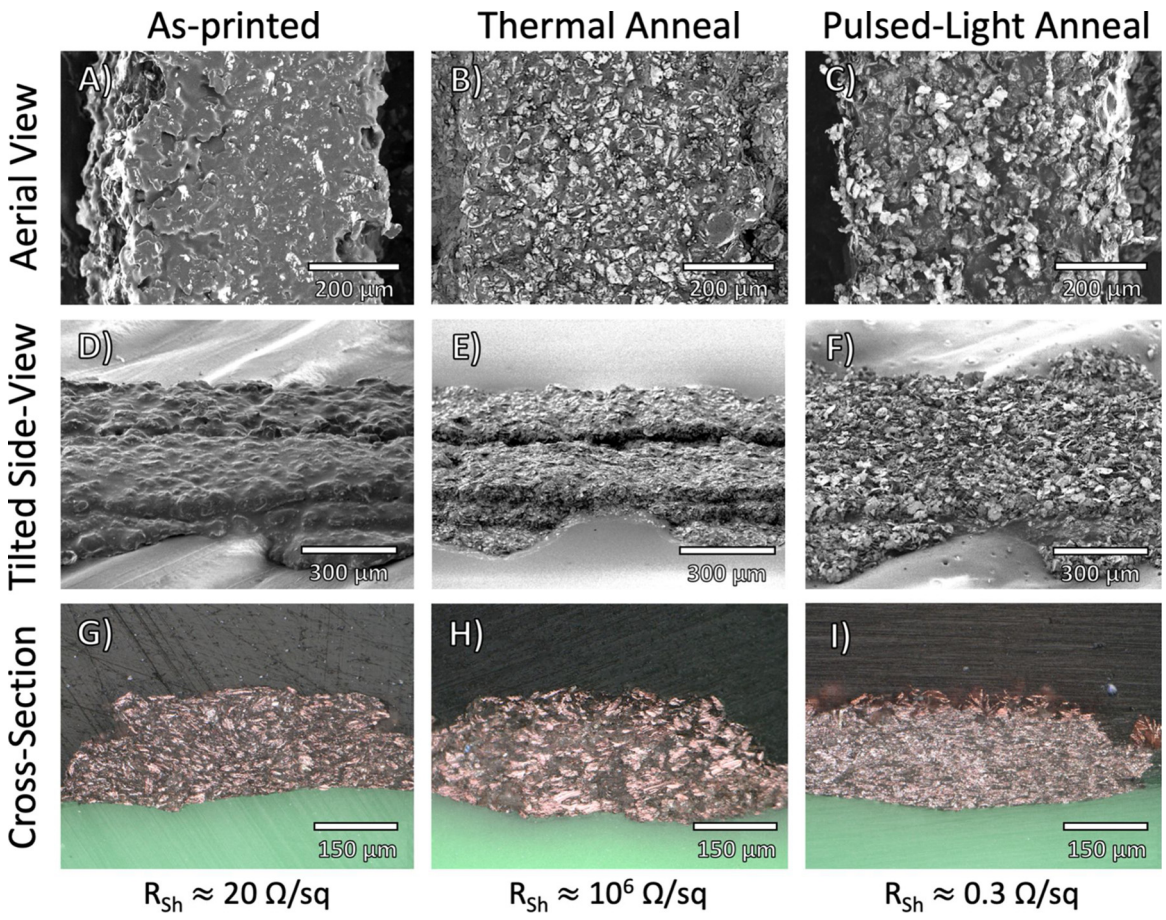

Fig. 2. SEM and optical analysis of conductive composite filament. A-C) SEM images of the surface of as-printed, thermally annealed, and pulsed-light annealed copper-loaded filament from an aerial view. D-F) SEM images of as-printed, thermally annealed, and pulsed-light annealed copper-loaded filament from a side view. G-I) Cross-sectional optical images of as-printed, thermally annealed, and pulsed-light annealed copper loaded filament cast in polished epoxy.

copper voids throughout the film, indicating that reflowing of the thermoplastic and copper-flake aggregation occurred, perhaps in addition to a small amount of shape retention after thermal expansion of the thermoplastic. In contrast, for the FAM samples the bulk of the exposed filament exhibited no such aggregation or expansion, while only showing thermoplastic ablation at the surface, suggesting that an extremely steep thermal gradient was imparted along the depth of the conductive filament by the pulsed-light for a very brief period of time.

X-ray photoelectron spectroscopy (XPS) was used to assess changes in surface composition across as-printed, exposed, and thermally cured samples (see XPS spectra in Supplementary Figure S3). While very little copper can be resolved in the XPS spectra of as-printed samples, the XPS spectra of exposed samples had clearly evident copper peaks, confirming exposed samples have a higher concentration of copper at the surface, which is consistent with the SEM images in Fig. 2. XPS spectra of the exposed samples also indicated the presence of other metals, such as silver, which is likely serving as a copper encapsulant to protect against oxidation at modest temperatures (as has been done in reference [26]). The presence of copper was also detected at the surface of thermally cured samples. However, large copper-oxide peaks were present in the XPS spectra of thermally cured samples, which suggests oxidation also plays a role in the thermal reduction of Electrifi's conductivity. For exposed samples, not only is the surface metal particle dense (as a result of thermoplastic vaporization), it is also free of metal-oxides, likely because the exposure process reduces copper oxide [38] and/or the high temperatures imparted by the exposure process do not last long enough for significant thicknesses of oxide to form.

To this point, all previously mentioned results were generated using high power density pulses. However, not all exposure parameters yielded the same or even beneficial results. Sheet resistance values for Electrifi samples exposed to a variety of pulse parameters are plotted in Fig. 3A-D as a function of capacitor bank voltage with calculated pulse profiles provided in the insets. Capacitor bank voltage is increased from 246 V to 450 V at various pulse widths ranging from 1 to 20 ms, resulting in exposures with emitted energy densities ranging from 0.5–25 J/cm^2. Generally, it can be seen that low energy density exposures actually increase Electrifi's sheet resistance, likely due to the low-intensity pulses only heating the surface, in a similar fashion to thermal annealing. However, as pulse energy density is increased, the sheet resistance begins to drop corresponding to ablation of thermoplastic, rather than just heating, until the sheet resistance begins to drop below that of the as-printed samples. Another general trend that should be noted is that larger pulse widths yield lower sheet resistance values at a constant bank voltage due to the increase in energy density that is emitted as a result of longer exposure times. However, decrements in sheet resistance diminished at larger pulse widths, due to strong pulse power density decay over longer periods of time. Although it was found that a capacitor bank voltage of 450 V (which is the maximum of the PulseForge® 1200) and a pulse width of 20 ms yielded the best results in sheet resistance, we postulate that higher capacitor bank voltages, corresponding to larger lamp power densities and higher light intensities could produce even better results.

As was shown in Fig. 2 and Figure S1, high-intensity pulsed light exposure ablated the topmost layer of filament thermoplastic and left behind a copper-dense surface while the underlying body of the filament remained unaffected. This observation is reflected in sheet resistance measurements of printed Electrifi films of various thicknesses shown in Fig. 3E. Electrifi was printed at a layer height of 0.1 mm,

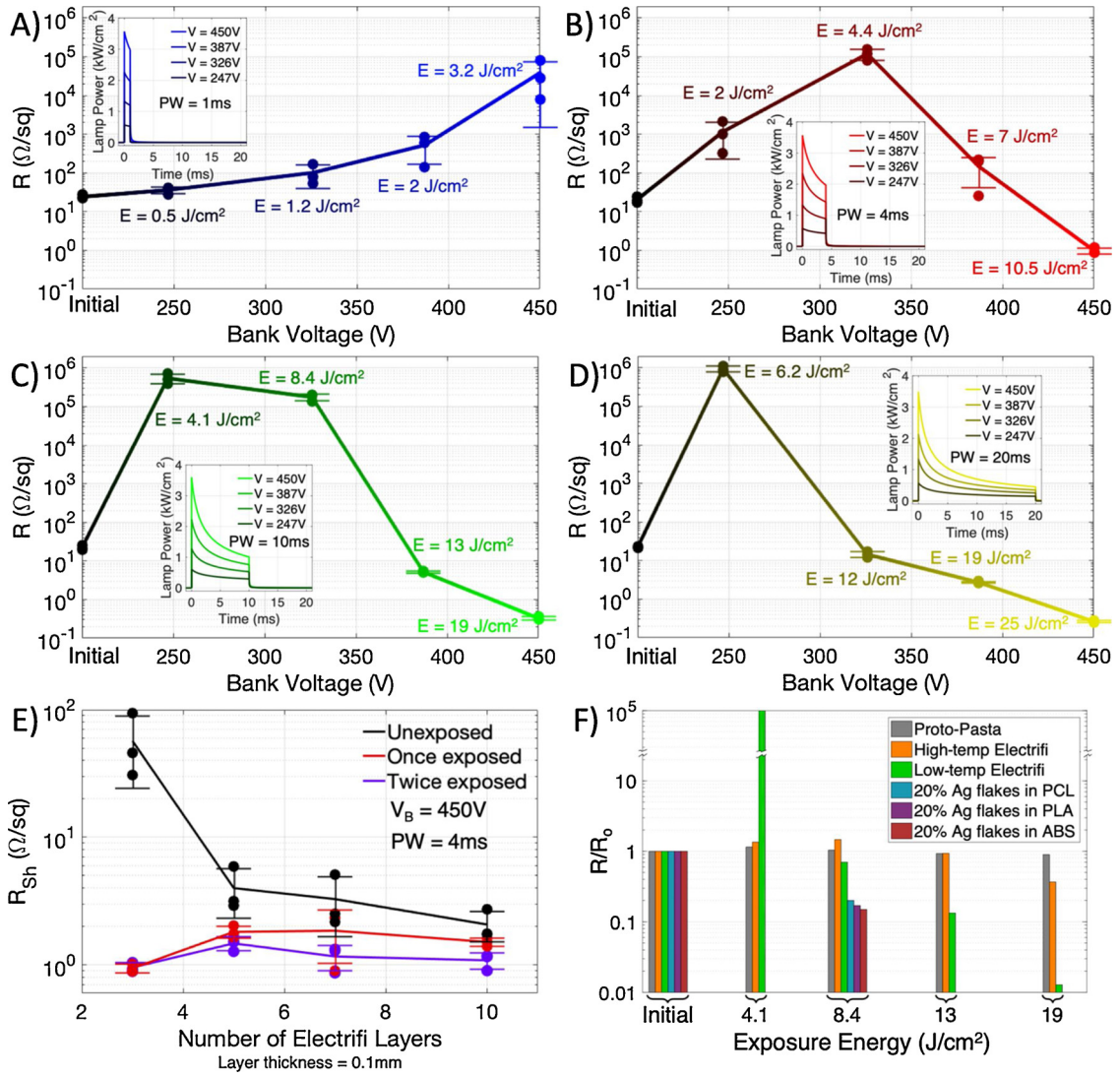

Fig. 3. Electrical characterization of pulsed-light exposed 3D printed filament. A-D) Sheet resistance of 3D-printed Electrifi with varying exposure conditions (bank voltage, pulse width) with pulse profiles provided in the insets. E) Sheet resistance plotted with an increasing number of printed Electrifi layers for unexposed, once-exposed and twice-exposed films. F) Sheet resistance comparison across various conductive filaments and exposure conditions.

corresponding to layer thickness values ranging from approximately 0.3 mm–1 mm. At its thinnest, 3 layers were needed to reliably produce continuous films on printed ABS substrates. It can be seen from Fig. 3E that, prior to exposure, there is a drop in film sheet resistance corresponding to an increasing number of printed layers. In contrast, the sheet resistance after exposure to high-intensity pulses is nearly thickness independent. This indicates that, electrically, almost all effects of pulsed-light exposure take place at the surface. Because the topmost 10 − 50 μm of thermoplastic is ablated, ideally, the 3D printer layer height would be set to within this range and pulsed-light exposure would occur on a layer-by-layer basis so that the high conductivity of the copper surface could be taken advantage of with increasing layers. However, due to manually moving the samples from printer to Pulseforge®, re-alignment issues, and restrictions in available printing equipment, no layer-by-layer exposures were carried out in this work, although there is equipment currently on the market equipped with built in FFF nozzles and a Pulseforge® lamp that could potentially be capable of carrying out layer-by-layer exposures [39].

There are currently a number of conductive filaments on the market, as summarized in Table S1, with most relying on carbon-based particulate with the exception of the metal-based Electrifi filaments. Electrifi was chosen as the main focus of this work since the filament is several orders of magnitude more conductive than the alternatives; however, a representative carbon based filament (Protopasta Conductive PLA) was also tested to help understand the effects of the process on the other main class of conductive filaments. To show how FAM impacts various filament compositions, a number of other conductive filaments and custom-made composite thermoplastics were also exposed to high intensity pulsed-light. Two additional filaments were tested including a high-temperature commercial carbon-loaded filament from Proto-Pasta, and a high-temperature version of Electrifi, whose thermoplastic consists of olefin block copolymers (OBCs). Both were subjected to similar exposure conditions as the standard Electrifi filament. All filaments exhibited similar responses to exposure conditions in that their sheet resistances increased at low exposure energies then began to decrease at high exposure energies, which can be seen in Fig. 3F. However, it should be noted that flash exposure had very little effect on the carbon-loaded filament, Proto-Pasta. High energy exposure of this filament left a plume of soot in the sample chamber thick enough to coat the lamp window, suggesting that both thermoplastic and carbon black were both ablated off of the sample surface upon exposure.

To determine whether the FAM process would be compatible with composite thermoplastics consisting of other metals, custom silver-loaded composites consisting of silver flakes dispersed at 20 % v/v in

ABS, polylactide (PLA), and polycaprolactone (PCL) were prepared via solution-casting with film thicknesses ranging from 0.3 – 0.5 mm. As shown in Fig. 3F, after an 8.4 J/cm^2 exposure the resistance of all three custom composites dropped to 20 %, 17 %, and 15 % of their original value for PCL, PLA, and ABS, respectively. The clear drop in resistance exhibited by all three custom-made composites indicates that thermoplastic has been ablated off the top surface, similar to what was observed with Electrifi (verified using before/after EDS images of the ABS samples, which can be seen in Supplementary Figure S4). Though the inclusion of these results in Fig. 3F is limited, they show that a variety of composite thermoplastic compositions responded well to flash light exposure, in that their sheet resistance dropped and their surfaces were metallized in a similar fashion to Electrifi. This suggests that the FAM process can likely be used to enhance many metal-composite filament compositions, potentially including any future commercial embodiments.

To assess the effects of part orientation during exposure, samples consisting of three 4-point Kelvin probe structures were placed under the PulseForge® lamp window at varying angles and proximities then exposed to pulsed light at a constant capacitor bank voltage of 450 V and a pulse width of 4 ms. With regards to proximity, a minimum in sheet resistance was measured, as shown in Fig. 4A, at a sample-to-lamp window distance of 15 – 20 mm corresponding to a focusing of light at that location. Samples were then twice exposed, resulting in a marginal reduction in resistance at almost all exposure proximities, however, there was again an optimal change in resistance at a sample proximity of 15 – 20 mm after the second pulse. At larger proximities, sample sheet resistance began to increase with an increasing number of pulses in a similar manner to the results of low-energy exposures, as shown in Fig. 3, which corresponded to surface heating rather than thermoplastic ablation. Aside from sheet resistance, there were also changes in sample color and texture, which can be seen in the inset images of Fig. 4A, with samples exposed at low lamp proximities having a course, more diffuse surface finish (corresponding to a copper-flake-rich surface) and samples exposed at larger lamp proximities having a more lustrous surface (corresponding to a thermoplastic-rich surface).

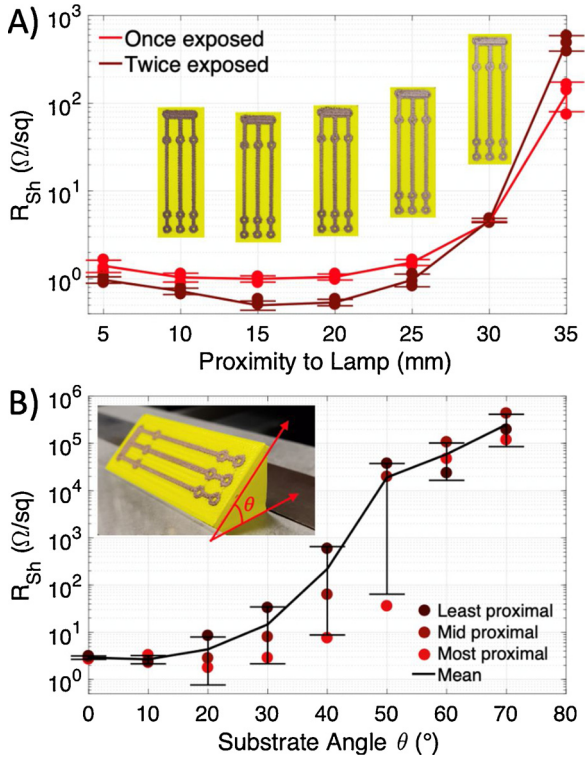

Fig. 4. Exposure effects associated with part orientation. A) Plot of sheet resistance versus part proximity from lamp window with optical images provided in the insets indicating color changes as part is moved away from lamp at a constant exposure condition (V = 450 V, PW = 4 ms). B) Plot of sheet resistance versus part angle with colored data points indicating which 4-point probe structures were closest to or furthest from the lamp during exposure (V = 450 V, PW = 4 ms).

Parts were also exposed at a variety of angles, result of which are displayed in Fig. 4B. These samples were placed in the Pulseforge® at a proximity of 30 mm (to ensure clearance at 90° angles), then exposed at progressively larger angles ranging from 0° to 80°. At a 0° exposure, the sample sheet resistance matches up well with what was measured in Fig. 4A. Generally, it was observed that the part sheet resistance is highly dependent on the exposure angle. However, the variance in sheet resistance across the three 4-point structures began to diverge at larger exposure angles, corresponding to a larger variance in proximity across the three structures. In fact, the most proximal 4-point structure on the sample (that is, the 4-point structure residing at the top of the angled part, whose data points are colored in bright red in Fig. 4B) became marginally less resistive at low exposure angles but drastically increased at higher exposure angles despite the further reduction in proximity to the lamp. From these results, it can be concluded that it is permissible to expose samples at low exposure angles (0°-20°), even if the sample is non-planar, as long as the part is small enough to be confined within the lamp's depth of focus, but flat exposure at a 15 – 20 mm proximity is optimal.

Although the most favorable embodiment of pulsed-light exposure to 3D-printed parts would take place in a layer-by-layer manner, the exposure process demonstrated in this work was still found to be suitable for enhancing the performance and reliability of 3D printed circuit boards (PCBs). To demonstrate the versatility of a 3D PCB process and its compatibility with pulsed-light exposure, an non-planar LED circuit was constructed on ABS, where the out-of-plane region consisted of the top fourth of a dome with a 2 cm radius of curvature, as shown in Fig. 5A and B. Electrifi was used to print two interconnect pathways with the first going up and over the dome and the second circumventing the dome and staying in-plane. Two samples of this design were prepared, the first without pulsed-light exposure and the second with exposure to a 10 ms, 450 V (19 J/cm^2) pulse with the sample stage set to a height such that the top of the dome had a 15 mm proximity to the lamp window. Two LEDs were then placed into sockets left in the 3D-printed substrate and silver paste was used to hold them in place. With a supply voltage of 2 V applied to the interconnect leads, the LEDs on the unexposed 3D PCB dimly lit, as shown in Fig. 5A, and the total current running through the circuit amounted to 0.16 mA. In contrast, the LEDs on the exposed 3D PCB lit brightly, as shown in Fig. 5B, and the total current running through the exposed circuit was 1.1 mA, indicating that the trace resistance had dropped significantly. However, it should be noted that the in-plane interconnect was less resistive, resulting in a slightly brighter in-plane LED. The higher resistance in the out-of-plane interconnects result from a non-zero exposure angle in addition to the vertical steps in the film associated with the layer-by-layer nature of FFF.

An oscillator circuit was also constructed onto a 3D PCB to demonstrate that pulsed-light processing is suitable for enhancing more complex electronics. A 555 timer astable oscillator circuit, a common timer circuit often used to demonstrate 3D printed electronic systems as in references [40], oscillates based on a resistor-capacitor exponential decay to switch between high and low voltages. In this demonstration, the output of the oscillator is used to blink a surface mounted LED. Two 3D PCBs were again prepared with and without exposure to a 10 ms, 450 V (19 J/cm^2) pulse. However, the layout of the 3D PCB was designed such that the output frequency of the LED would depend on the resistance of a printed resistor R_1, which is visible in the image of the circuit layout shown in Fig. 5C. The value of R_2 and C_1 were selected such that the differences in frequency and duty cycle of the output waveforms between the exposed and unexposed samples would be

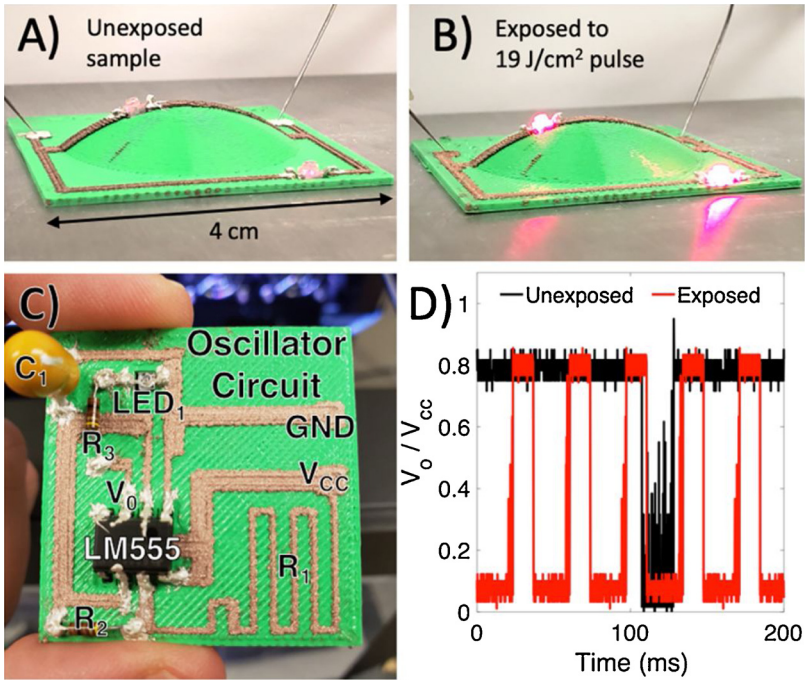

Fig. 5. Pulsed-light exposed 3D printed circuit boards. A-B) Images of non-planar LED circuits driven at 2 V a) without and b) with pulsed-light exposure. C) Image of a 3D printed oscillator circuit board and interconnects with placed-in components adhered with silver epoxy. D) Output signal (V_o/V_{cc}) waveform of oscillator circuits prepared with and without pulsed-light exposure.

visibly and obviously apparent. A schematic diagram of the 3D PCB 555 timer oscillator circuit is shown in Supplementary Figure S5. The output waveform from each circuit is plotted in Fig. 5D, with the exposed output colored in red and the unexposed output colored in black. The output frequency of the exposed and unexposed samples was 26 Hz and 6 Hz, respectively, the differences of which were visibly apparent, corresponding to a substantial drop in the resistance of R_1 after FAM exposure. A slow-motion video of the two circuits operating is shown in Supplementary Video 1. In addition to higher frequency, the stability of the exposed circuit was much better than that of the unexposed circuit, whose frequency was varying considerably over time. The unexposed circuit also required a larger supply voltage in order to properly operate, due to a larger voltage drop over its more resistive interconnects. The notable differences in performance, reliability and circuit stability of the pulsed-light exposed 3D PCBs points to the already practical effectiveness of FAM processing.

The work demonstrated here is a promising method for improving the electrical performance of metal-composite parts used in larger scale industrial 3D printers for rapid and relatively low cost production of custom parts. Additionally, in the long-term, there is a potential for the integration of pulsed lamps within printers for the lower-cost hobbyist markets. The ideal configuration of a pulsed-light setup on a 3D printer would be one that is carried out in-line with the printing process, in a similar fashion to how poly-inkjet 3D printers utilize ultraviolet light to photopolymerize consecutively printed layers, [41] so that photonic processing can be carried out layer-by-layer and completely autonomously. To this end, further study is needed with specialty equipment to develop an in-line printing process and determine to what degree multi-exposed films are enhanced. Although broadband, large-area pulsed-light exposure from a flash lamp is shown in this work to be highly effective for enhancing conductive composite filaments, our results also implicate the potential for high-power lasers to do the same, which could potentially be a cheaper alternative. Additionally, a more detailed investigation of various thermoplastics' interaction and response to high-intensity light is needed, so that perhaps the thermoplastic's polymer makeup and the light's wavelength, polarization, and intensity can carefully selected to produce a desired outcome. The FAM technique can also potentially be used to enhance composite thermoplastics in applications outside of additive manufacturing, such as EMI shielding or heat dissipation. Overall, we believe that the discoveries presented in this work reveal a large-scale potential for the photonic processing of conductive thermoplastics and represents a significant advancement toward the development and widespread use of 3D printed electronics.

3. Conclusion

In summary, we have demonstrated flash ablation metallization (FAM), a process that involves the use of high-intensity pulsed light to enhance conductive composite thermoplastics and produce films that are up to two orders of magnitude more conductive than as-prepared films. This is demonstrated in contrast to thermal curing, a process that yields a higher resistance for conductive composite thermoplastics. The FAM process was found to generally enhance a variety of conductive thermoplastics. Through SEM and cross-sectional optical images, it was found that filament enhancement is attributed to ablation of thermoplastic at the surface of the filament, which left behind a metallized surface layer while leaving an underlying 3D printed ABS substrate structurally unaffected. 4-point resistance measurements were used to assess changes in conductivity in a variety of filaments, where it was found that longer, higher energy exposures generally yielded lower film resistances, and that the resistance after exposure was nearly thickness independent. Pulsed-light exposure was then demonstrated to enhance the performance and stability of 3D printed circuit boards, which is immediately relevant for 3D printed electronic applications. In addition to these advancements, the discovery that high intensity light can be used to enhance conductive filament reveals a larger-scale potential for the use of photonic processing in fused filament fabrication and in broader composite thermoplastic applications such as EMI shielding.

Data availability

All data needed to evaluate the conclusions in the paper are present in the paper and the Supplementary Materials. Additional data for this study are available from the corresponding author upon request.

Funding sources

J.A.C. acknowledges support from the National Science Foundation (NSF) through the NSF graduate research fellowship (grant no. DGE11010101-0417-7172-7172/4103) and support from Oak Ridge Associated Universities (ORAU) at Army Research Laboratory (grant no. W911NF-16-2-0008). This work was supported by internal funds from the US Army Research Laboratory. This work was performed in part at the Duke University Shared Materials Instrumentation Facility (SMIF), a member of the North Carolina Research Triangle Nanotechnology Network (RTNN), which was supported by the National Science Foundation (Grant ECCS-1542015) as part of the National Nanotechnology Coordinated Infrastructure (NNCI).

CRediT authorship contribution statement

Jorge A. Cardenas: Conceptualization, Investigation, Methodology, Formal analysis, Writing - original draft. **Harvey Tsang:** Conceptualization, Investigation, Methodology, Resources, Supervision. **Huayu Tong:** Investigation, Methodology. **Hattan Abuzaid:** Investigation, Formal analysis, Writing - review & editing. **Katherine Price:** Investigation, Formal analysis. **Mutya A. Cruz:** Investigation, Methodology. **Benjamin J. Wiley:** Conceptualization, Resources, Supervision, Writing - review & editing. **Aaron D. Franklin:** Conceptualization, Resources, Writing - review & editing. **Nathan Lazarus:** Conceptualization, Investigation, Methodology, Resources, Supervision, Writing - review & editing.

Declaration of Competing Interest

B.J.W. has an equity interest in Multi3D LLC, the manufacturer of Electrifi filament.

Acknowledgements

The authors would like to thank Allen Gray and Shengrong Ye from Multi3D LLC for supplying their high temperature Electrifi filament.

Appendix A. Supplementary data

Supplementary material related to this article can be found, in the online version, at doi:https://doi.org/10.1016/j.addma.2020.101409.

References

[1] T.D. Ngo, A. Kashani, G. Imbalzano, K.T.Q. Nguyen, D. Hui, Compos. Part B Eng. 143 (2018) 172.
[2] B.-H. Lu, H.-B. Lan, H.-Z. Liu, Opto-Electronic Adv. 1 (2018) 17000401.
[3] A.D. Valentine, T.A. Busbee, J.W. Boley, J.R. Raney, A. Chortos, A. Kotikian, J.D. Berrigan, M.F. Durstock, J.A. Lewis, Adv. Mater. (2017) 29, https://doi.org/10.1002/adma.201703817.
[4] R.D. Farahani, M. Dubé, D. Therriault, Adv. Mater. (2016) 5794.
[5] J. Odent, T.J. Wallin, W. Pan, K. Kruemplestaedter, R.F. Shepherd, E.P. Giannelis, Adv. Funct. Mater. 27 (2017), https://doi.org/10.1002/adfm.201701807.
[6] E. MacDonald, R. Wicker, Science 80- (2016) 353, https://doi.org/10.1126/science.aaf2093.
[7] Y. Gu, D. Park, D. Bowen, S. Das, D.R. Hines, Adv. Mater. Technol. (2019) 4, https://doi.org/10.1002/admt.201800312.
[8] S.Y. Wu, C. Yang, W. Hsu, L. Lin, Microsyst. Nanoeng. 1 (2015), https://doi.org/10.1038/micronano.2015.13.
[9] Y. Dong, C. Bao, W.S. Kim, Joule 2 (2018) 579.
[10] H.H. Lee, K. Sen Chou, K.C. Huang, Nanotechnology 16 (2005) 2436.
[11] K. Park, D. Seo, J. Lee, Colloids Surfaces A Physicochem. Eng. Asp. 313–314 (2008) 351.
[12] Q. Li, J.A. Lewis, Adv. Mater. 15 (2003) 1639.
[13] M. Singh, H.M. Haverinen, P. Dhagat, G.E. Jabbour, Adv. Mater. 22 (2010) 673.
[14] X. Cao, C. Lau, Y. Liu, F. Wu, H. Gui, Q. Liu, Y. Ma, H. Wan, M.R. Amer, C. Zhou, ACS Nano 10 (2016) 9816.
[15] J.A. Cardenas, J.B. Andrews, S.G. Noyce, A.D. Franklin, Nano Futur. 4 (2020) 012001.
[16] X. Wang, M. Jiang, Z. Zhou, J. Gou, D. Hui, Compos. Part B Eng. 110 (2017) 442.
[17] “Electrifi conductive filament", Multi3D,” can be found under https://www.multi3dllc.com/, n.d. 7/1/2020.
[18] "Proto-pasta electrically composite PLA," Protoplant," can be found under https://www.proto-pasta.com/products/conductive-pla, n.d. 7/1/2020.
[19] P.F. Flowers, C. Reyes, S. Ye, M.J. Kim, B.J. Wiley, Addit. Manuf. 18 (2017) 156.
[20] M.J. Kim, M.A. Cruz, S. Ye, A.L. Gray, G.L. Smith, N. Lazarus, C.J. Walker, H.H. Sigmarsson, B.J. Wiley, Addit. Manuf. 27 (2019) 318.
[22] Y. Xie, S. Ye, C. Reyes, P. Sithikong, B.I. Popa, B.J. Wiley, S.A. Cummer, Appl. Phys. Lett. 110 (2017), https://doi.org/10.1063/1.4982718.
[23] M.L. Clingerman, J.A. King, K.H. Schulz, J.D. Meyers, J. Appl. Polym. Sci. 83 (2002) 1341.
[24] S.Y. Pak, H.M. Kim, S.Y. Kim, J.R. Youn, Carbon 50 (2012) 4830.
[25] S.J. Leigh, R.J. Bradley, C.P. Purssell, D.R. Billson, D.A. Hutchins, PLoS One 7 (2012), https://doi.org/10.1371/journal.pone.0049365.
[26] M.A. Cruz, S. Ye, M.J. Kim, C. Reyes, F. Yang, P.F. Flowers, B.J. Wiley, Part. Part. Syst. Charact. 35 (2018), https://doi.org/10.1002/ppsc.201700385.
[27] "BlackMagic conductive graphene PLA filament." BlackMagic3D. http://www.blackmagic3d.com/Conductive-p/grphn-pla.htm, n.d. 7/1/2020.
[28] "Our flexible hybrid electronic materials." ACI Materials.https://www.acimaterials.com/applications/flexible-hybrid-electronics/, n.d. 7/1/2020.
[29] "Metalon conductive inks." NovaCentrix. https://www.novacentrix.com/products/metalon-conductive-inks, n.d. 7/1/2020.
[30] K. Gnanasekaran, T. Heijmans, S. van Bennekom, H. Woldhuis, S. Wijnia, G. de With, H. Friedrich, Appl. Mater. Today 9 (2017) 21.
[31] K. Angel, H.H. Tsang, S.S. Bedair, G.L. Smith, N. Lazarus, Addit. Manuf. 20 (2018) 164.
[32] J.R. Jian, T. Kim, J.S. Park, J. Wang, W.S. Kim, AIP Adv. 7 (2017), https://doi.org/10.1063/1.4979173.
[33] K.A. Schroder, S.C. McCool, W.F. Furlan, NSTI-Nanotech 2006, Nano Science And Technology Institute, 2006, p. 198.
[34] J. Niittynen, E. Sowade, H. Kang, R.R. Baumann, M. Mäntysalo, Sci. Rep. 5 (2015), https://doi.org/10.1038/srep08832.
[35] S. Das, D. Cormier, S. Williams, Procedia Manuf. Elsevier B.V., 2015, pp. 366–377.
[36] “Pulseforge® 1200," NovaCentrix. https://www.novacentrix.com/products/pulseforge/1200, n.d. 7/1/2020.
[37] M.J. Guillot, S.C. McCool, K.A. Schroder, ASME Int. Mech. Eng. Congr. Expo. Proc., American Society Of Mechanical Engineers Digital Collection, (2012), pp. 19–27.
[38] H. Kang, E. Sowade, R.R. Baumann, ACS Appl. Mater. Interfaces 6 (2014) 1682.
[39] “3D Printed Electronics too" NovaCentrix.” https://www.novacentrix.com/products/pulseforge/3d-fabrication, n.d. 7/1/2020.
[40] J. Li, Y. Wang, G. Xiang, H. Liu, J. He, Adv. Mater. Technol. 4 (2019), https://doi.org/10.1002/admt.201800529.
[41] M. Layani, X. Wang, S. Magdassi, Adv. Mater. 30 (2018), https://doi.org/10.1002/adma.201706344.